A CMOS-MEMS Lateral-axis Gyroscope

Huikai Xie* and Gary K. Fedder*†
*Department of Electrical and Computer Engineering and †The Robotics Institute
Carnegie Mellon University, Pittsburgh, PA 15213
Email: xie@ece.cmu.edu; Tel: (412) 268-6607; Fax: (412) 268-4595

ABSTRACT

This paper reports on the experimental results from the first design of a CMOS lateral-axis vibratory gyroscope that utilizes comb fingers for both actuation and sensing. The fabrication is compatible with standard CMOS processes and the design has an integrated, fully-differential capacitive interface circuit. This gyroscope design uses integrated comb drives for out-of-plane actuation, and is motivated by the desire to integrate three-axis gyroscopes on a single chip. The packaged gyroscope operates at atmospheric pressure with a sensitivity of 0.12 mV/deg/s and the resonant frequency of the drive mode is thermomechanically tuned between 4.2 - 5.1 kHz. Resonant frequency matching between the drive and sense modes is realized by integrating a polysilicon heater inside the spring beams.

INTRODUCTION

Recently, markets in automotive and consumer electronic products are demanding low-cost gyroscopes for driving security and comfort, and motion stability control. Micromachined gyroscopes are the potential candidates because of their batch fabrication, small size, possibility of integrating signal processing circuits, and multi-axis integration. A recent study shows that the market for micromachined gyroscopes in automotive industry alone will be about US$0.5 billion by 2003 [1].

After the first silicon micromachined gyroscope was proposed by Draper Lab in 1991 [2], various fabrication technologies, structural designs and drive/sense mechanisms for micro-gyroscopes have been investigated [3,4,5,6]. Generally speaking, bulk micromachined gyroscopes have large mass but no on-chip read-out electronics and require Si-Si and/or Si-glass anodic bonding and two-side alignment. Surface micromachined gyroscopes have integrated read-out electronics but small mass, and they suffer from thin-film residual stress, squeeze-film damping and sacrificial layer release problems. Combination of the two micromachining processes, or mixed technology, is also being explored. Bosch reported in 1997 a yaw rate gyro fabricated by using the combination of bulk and surface micromachining [5]. Samsung achieved 0.015 °/s at 25 Hz bandwidth by using a mixed technology [6]. However, the current mixed technology still suffers from sacrificial layer release and squeeze-film damping problems and often requires expensive SOI wafers.

The CMOS-MEMS process developed at Carnegie Mellon University is a maskless, post-CMOS process in which the etching masks are provided by the interconnect metal layers in the standard CMOS process [7]. The cross-sectional view of the final step of the CMOS-MEMS process is illustrated in Figure 1. This process can be used to fabricate microstructures with high aspect-ratio, large gap to the substrate, high flexibility of wiring and dry etching for release. Structures have no sticking problem and small squeeze-film damping of the out-of-plane modes. Curling from residual stress gradients in the composite films can be compensated to the first order via a curl matching frame [8]. This process has been used to fabricate both lateral-axis and z-axis accelerometers and z-axis gyroscopes [8,9,10]. A lateral-axis gyroscope is still needed to complete an integrated inertial measurement unit (IMU) with six degrees-of-freedom.

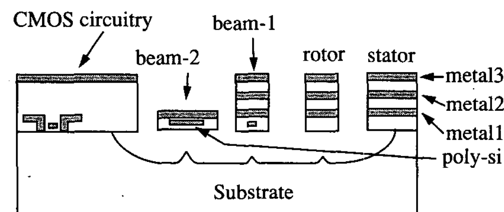

Figure 1. Schematic cross-section of the last step of the post-CMOS micromachining process.

A significant advantage of the CMOS-MEMS process is that out-of-plane actuation and displacement-sensing can be easily realized [9,11]. This paper mainly focuses on implementation of the out-of-plane actuation for design of lateral gyroscopes. Experimental results on motion sensing and mode coupling are presented. A method of thermomechanically tuning resonance frequency for mode matching is also proposed and experimentally verified. In addition, a special beam design is proposed to compensate lateral curling.

OUT-OF-PLANE ACTUATION PRINCIPLE

As shown in Fig. 1, microstructures can consist of up to three metal layers, which is a major difference from homogeneous polysilicon counterparts. These multi-conductor layer structures make it possible to construct multiple capacitors between comb fingers. There are 22 different voltage configurations for combs with 3 metal layers that provide vertical actuation.

The cross-section of the comb fingers used for vertical actuation is shown in Fig. 2(a). The comb fingers have two or three metal layers and are located about 25 μm above the substrate, which leaves enough room for z-motion. This large gap is also an advantage for capacitive comb-finger sensing because the parasitic capacitance to the substrate is greatly reduced. All three metal layers in the rotor are electrically connected while the metal-1 and metal-3 in the stator are separately connected. Two sidewall capacitors, C_1 and C_2, are formed, as shown in Fig. 2(a). If a voltage is applied across C_1 or C_2, the rotor will move in the z-direction and the device operates as a z-axis actuator.

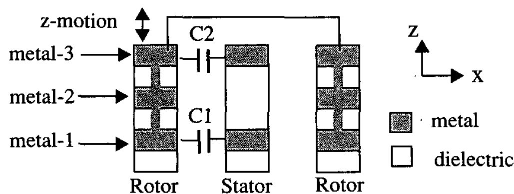

Figure 2(a). Cross-section and wiring configuration for z-axis actuation and position-sensing.

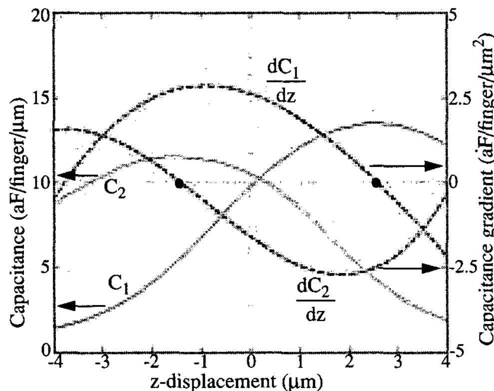

Figure 2(b). Capacitance and capacitance gradient vs. z-displacement.

In order to evaluate the capacitance and expected displacement, a finite element analysis tool, the Maxwell 2D field simulator [12], is employed. The calculated C_1 and C_2 and their gradients versus z-displacements are shown in Fig. 2(b). Note that the maximum static displacement range is defined by the intersections of the two gradient curves with the zero-gradient line in Fig. 2(b). The intersections are located at -1.4 μm and 2.6 μm.

SENSOR DESIGN AND FABRICATION

A lateral-axis microgyroscope needs either vertical actuation or vertical motion sensing. Considering the practical issues, such as the mismatch between rotor and stator fingers and the requirement of curl matching frames, vertical actuation as described in the previous section is employed.

The topology of the proposed gyroscope is shown in Fig. 3, which includes three key components: a z-axis comb-drive, a y-axis accelerometer, and a z-axis position sensor used for feedback control of the z-axis actuation. There are 180 comb fingers for z-axis actuation and 200 comb fingers for y-axis acceleration sensing. The rotation sense axis of this device is along the x-axis. A y-axis actuator is also included inside the embedded y-axis accelerometer to compensate the off-axis motion coupled from the z-axis excitation vibration. Note that for the sensors, four groups of comb fingers form a common-centroid configuration to reduce the influence of process variation and cross-axis sensitivities.

Mode coupling, sensitivity, and multi-axis integration depend on spring design. Ideally, each spring should have only one degree-of-freedom. However, springs are constructed from beams with finite values of spring constants in all directions. This is one of the major sources of mode coupling. In reality, the stiffness in the

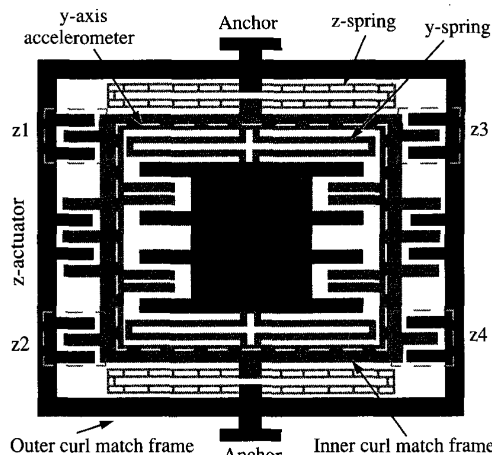

Figure 3. Topology of the lateral-axis gyroscope.

primary mode should be at least one order of magnitude smaller than any other modes to separate the primary mode from other modes and reduce the secondary off-axis motion.

Note that, in Fig. 1, beam-2 is thinner than beam-1. Indeed, the CMOS-MEMS process provides beams with different thicknesses by choosing different interconnect metal layers as the etching mask. Typically, beams with Metal_1, Metal_2, Metal_3 on the top are 1.9 μm, 3.5 μm, 5.0 μm thick, respectively. Fig. 4 shows the spring designs for x- and z- axes. A z-compliant spring is realized by connecting multiple beams with short trusses and using beams with Metal_1 on the top. The lateral-compliant spring is realized by using narrow beams. Assuming the beam width is 1.5 μm and the beam thickness is 5.0 μm, the x-stiffness will be about one order smaller than the z-stiffness.

Another design issue with springs is the lateral curling of spring beams, which results in lateral position offset [8]. This lateral curling is believed to be caused by the asymmetric cross-section of the spring beams. The cross-sectional asymmetry results from the process variations, especially from photolithography misalignment. For example, suppose we have a beam composed of metal-1, metal-2 and metal-3. The three metal layers are designed to have identical width and be completely overlapped. However, due to the finite precision of the photolithography, the metal layers will have certain misalignment. Since all metal layers can function as the structural etching mask, oxide will fill the vacancy left by the metal-2 shift, as shown in Fig. 5(a). Lateral curling becomes worse as beam thickness decreases. In order to reduce this lateral curling, a special tapered beam is proposed. As shown in Fig. 5(b),

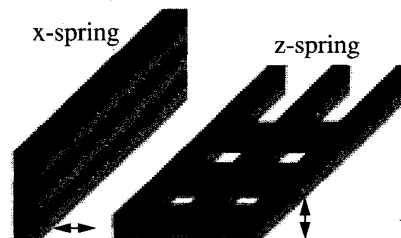

Figure 4. Spring designs.

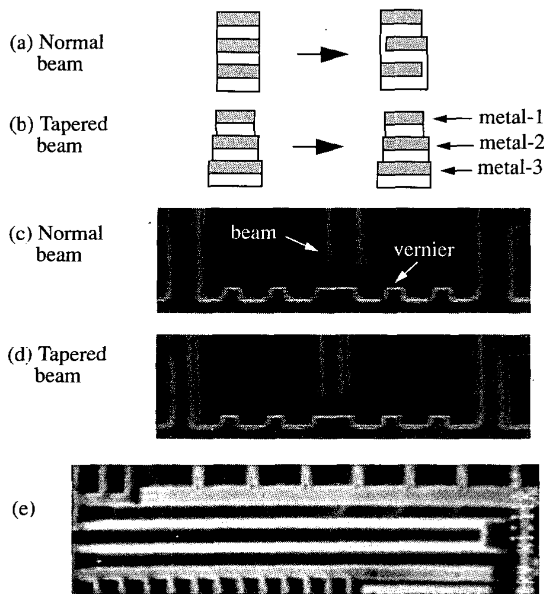

Figure 5. Lateral curling elimination. (e) a tapered y-spring demonstrating near perfect lateral alignment.

lower level metal layers are made wider. As long as the width difference is larger than the photolithography error, there will be no oxide remaining beside any metal layer. Fig. 5(c) and (d) shows SEMs of two released beams with a normal design and a tapered design, respectively. The beams have the same length of 160 μm. It is obvious that the tapered beam significantly reduces the lateral curling. Fig. 5(e) is SEM of a y-axis spring with a tapered design, in which no lateral curling is observed.

The device is fabricated in the Hewlett-Packard 0.5 μm CMOS process followed by a two-step post-CMOS micromachining process. First, an anisotropic reactive-ion-etch (RIE) of dielectrics by using CHF_3/O_2 plasma is performed to define the microstructures. Second, a deep silicon RIE is performed by using SF_6 plasma, followed by an isotropic silicon undercut to release

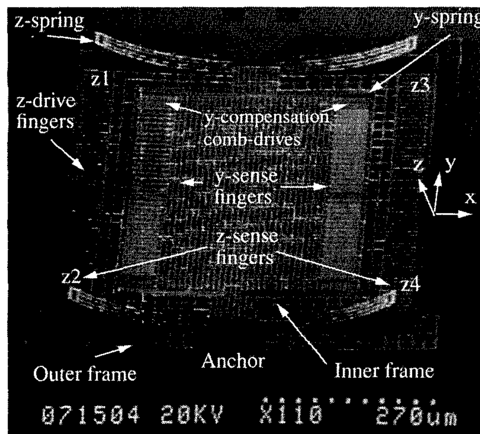

Figure 6: SEM of a released gyroscope.

the microstructures. The isotropic etch is achieved by greatly reducing the platen power. Fig. 6 shows an SEM of a released gyroscope.

CHARACTERIZATION

As shown in Fig. 6, the ends of the z-spring beams curl up 70 μm due to the residual stress and thermal coefficient mismatch in the embedded layers inside the beams. This curling can be compensated by injecting a current through a polysilicon resistor inside the spring beams [13]. With the aid of a MIT Microvison System [14], it was observed that flattening of the spring beams increases the suppression of the mode coupling and changes the resonant frequency of the drive mode (Fig. 7(b)). Meanwhile the resonance of the sense mode stays almost unchanged. Therefore, the integrated heater provides an alternative method to match the resonant frequency between the sense and drive modes if necessary. The measured dependence of resonant frequency of the drive mode to the heater current is shown in Fig. 7(c). A rapid change occurs when the spring beams approach the curl matching state at a heater current of 1 mA.

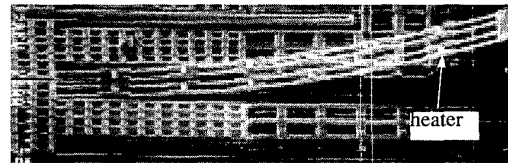

(a) SEM of a z-spring beam with a polysilicon heater.

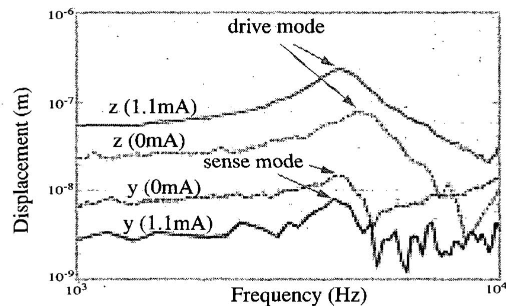

(b) Frequency responses of the drive and sense modes with and without injecting current.

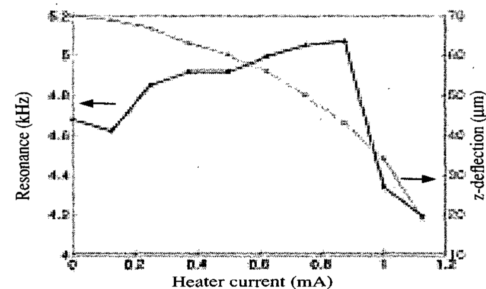

(c) Resonant frequency and z-deflection changes of the drive mode with respect to heating

Figure 7: Curling compensation and resonant frequency tuning by heating

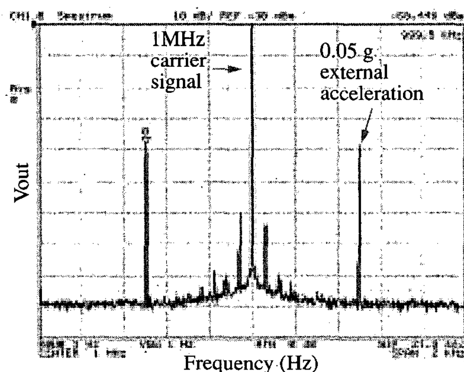

Figure 8: Spectrum of the y-accelerometer at a 500 Hz, 0.05 g external acceleration, showing a resolution of 100 μg/rtHz.

The embedded y-axis accelerometer detects the coupled motion and then feeds back to the integrated actuators to null the y-axis coupled motion at the zero rotation state. Because of the high flexibility of wiring provided by the CMOS-MEMS process, a fully-differential capacitive bridge is implemented. There is a differential input pair preamplifier integrated on the chip. A spectrum of the y-axis accelerometer response is plotted in Fig. 8 showing a resolution of 100 μg/rtHz. The rotation test result by using a turntable is shown in Fig. 9. The large DC offset is due to the remaining coupled motion. This test was performed in air with no current injected into the polysilicon heater to flatten the z-axis springs. Thus the coupled motion was large and drove the embedded y-axis accelerometer out of its linear range. Further test with coupled motion suppression by injecting current into the polysilicon heater and off-axis motion compensation by the integrated y-axis actuator is under investigation.

CONCLUSION AND FUTURE WORK

A lateral-axis CMOS-MEMS gyroscope with out-of-plane actuation is demonstrated. Thus, 3-axis gyro integration for a 6-DOF IMU can be implemented by using the CMOS-MEMS process. The proposed thermal tuning by using an integrated polysilicon heater can be used to match the drive and sense modes, and can also be used for temperature compensation. It is experimentally verified that tapered beams significantly reduce lateral curling.

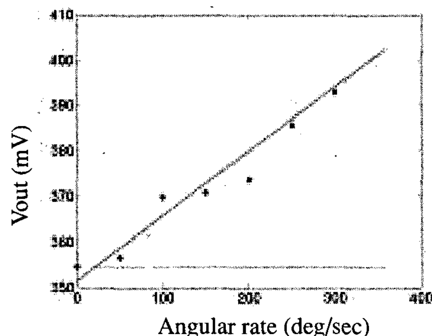

Figure 9: Constant rotational rate measurement. A large DC offset was present because of the coupled motion from the drive mode.

However, this gyroscope design is not optimized. The drive spring and sense spring are in parallel because of the curl matching. This arrangement cannot obtain a high y-axis stiffness ratio between the two springs, resulting in low mode coupling rejection. In the next generation, the two springs will be orthogonal to each other. A key issue will then be how to achieve appropriate curl matching.

ACKNOWLEDGEMENT

The authors would like to thank Hao Luo for circuit design. This work was sponsored by DARPA under the AFRL, Air Force Materiel Command, USAF, under agreement F30602-97-2-0323.

REFERENCES

1. System Planning Corporation, "MEMS 1999: Emerging Applications and Markets", *http://memsmarket.sysplan.com/study.html*, 1999.

2. P. Greiff, B. Boxenhorn, T. King, L. Niles, "Silicon monolithic micromechanical gyroscope", *Transducers '91*, San Francisco, CA, USA; 24-27 June 1991, pp.966-8

3. M. Putty, K. Najafi, "A micromachined vibrating ring gyroscope", *Tech. Digest Solid-State Sensor & Actuator Workshop*, Hilton Head Island, SC, USA; 13-16 June 1994, p213-20

4. W.A. Clark, R.T. Howe, R. Horowitz, "Surface micromachined Z-axis vibratory rate gyroscope", *Tech. Digest Solid-State Sensor & Actuator Workshop*, Hilton Head Island, SC, USA; 3-6 June 1996, p.283-7

5. M. Lutz, W. Golderer, J. Gerstenmeier, J. Marek, B. Maihofer, S. Mahler, H. Munzel, U. Bischof, "A precision yaw rate sensor in silicon micromachining", *Transducers'97*, Chicago, June 16-19, 1997, p.847-850.

6. K.Y. Park, H.S. Jeong, S. An, S.H. Shin, and C.W. Lee, "Lateral gyroscope suspended by two gimbals through high aspect ratio ICP etching", *Transducers'99*, Sendai, Japan, June 7-10, 1999, p.972-975.

7. G.K. Fedder *et al.*, "Laminated high-aspect-ratio micro-structures in a conventional CMOS process", *Sensors and Actuators A*, vol.A57, p.103-110.

8. G. Zhang, H. Xie, L. deRosset, G.K. Fedder, "A lateral capacitive CMOS accelerometer with structural curl compensation", *MEMS'99*, Orlando, FL, USA; 17-21 Jan. 1999, p606-611.

9. H. Xie, G.K. Fedder, "A CMOS z-axis accelerometer with capacitive comb-finger sensing", *MEMS 2000*, Miyazaki, Japan; 25-28 Jan. 2000, p496-501.

10. H. Luo, G.K. Fedder, L.R. Carley, "An ellastically gimbaled CMOS-MEMS gyroscope", *International Symposium on Smart Structure and Microsystem*, Oct. 19-21, 2000, HongKong, China

11. H. Xie, L. Erdmann, Q. Jing, G.K. Fedder, "Simulation and characterization of CMOS z-axis microactuator with electrostatic comb drives", *Proc. 2000 Int. Conf. on Modeling and Simulation of Microsystems*, San Diego, CA; 27-29 Mar. 2000, p181-184.

12. Maxwell 2D field simulation, Version 1.9.04, Copyright 1984-1997, Ansoft Corporation.

13. H. Lakdawala, G.K. Fedder, "Analysis of temperature-dependent residual stress gradients in CMOS micromachined structures", *Transducers '99*, Sendai, Japan, June 7-10 1999, p526-529.

14. W. Hemmert, M.S. Mermelstein and D.M. Freeman, "Nanometer resolution of 3-D motions using video interference microscopy", *MEMS'99*, p302-308.